

## Orientational ordering and the low temperature structure of SF<sub>6</sub>

by B. M. POWELL†, M. T. DOVE‡,  
G. S. PAWLEY§ and L. S. BARTELL||

† Atomic Energy of Canada Limited, Chalk River Nuclear Laboratories,  
Chalk River, Ontario, KOJ 1J0, Canada

‡ Department of Earth Sciences, University of Cambridge,  
Cambridge, CB2 3EQ, England

§ Department of Physics, University of Edinburgh,  
Edinburgh, EH9 3JZ, Scotland

|| Department of Chemistry, University of Michigan,  
Ann Arbor, Michigan 48109, U.S.A.

*(Received 5 June 1987; accepted 16 June 1987)*

The crystal structure of sulphur hexafluoride in its low temperature phase has been solved from neutron powder diffraction measurements. At both 23 K and 85 K the structure is triclinic, space group  $P\bar{1}$ , with  $Z = 3$ . It is in good agreement with the structure predicted previously by molecular dynamics simulations. No evidence was found for the existence of an hexagonal phase. The phase transition is interpreted in terms of two separate lattice distortions from the cubic, high temperature phase which couple to different stages of orientational ordering. The mechanism driving the transition is the resolution of orientational frustration as the temperature is reduced. The present results confirm the validity of the simple intermolecular force model employed in the simulations for SF<sub>6</sub> and they have been used to improve the parameters of this model.

### 1. Introduction

The existence of a phase transition in sulphur hexafluoride (SF<sub>6</sub>) was first indicated by calorimetric measurements [1]. The transition, at 96 K, was subsequently confirmed by N.M.R. measurements [2, 3], while a second transition at 45 K was suggested by the temperature dependence of the linewidths and second moments [3]. X-ray diffraction data [2] showed the high temperature phase to be bcc and probably orientationally disordered (OD). The detailed structure of this phase was determined by neutron diffraction measurements [4, 5]. These showed that the average orientation of the molecules has the S-F bonds lying along the cubic axes, but there are large mean square deviations from this average orientation. Extensive Molecular Dynamics Simulation (MDS) calculations [6-9] have shown that the origin of the disorder in SF<sub>6</sub> is associated with orientational frustration effects rather than the more common statistical disorder or large amplitude thermal fluctuations. Many of the properties of this phase (e.g. temperature effects, single molecule dynamics, collective excitations and the effects of rotation-translation coupling) are now reasonably well understood.

Despite this increased understanding of the high temperature OD phase, the determination of the crystal structure of the phase (or phases) below 96 K has remained an unsolved problem. Neutron powder diffraction data [10] indicated the structure to be of low symmetry and showed that it must be very similar at 20 K and 75 K. However, all efforts to find a set of unit cell parameters to match these diffraction data failed. Since these efforts included the use of exhaustive search methods [11] which would have identified a cell of monoclinic or higher symmetry, this implied that the structure of SF<sub>6</sub> below 96 K is probably triclinic at all temperatures. On the other hand, electron diffraction data [12] obtained between 45 K and 96 K could be analysed in terms of an hexagonal unit cell containing three molecules. The hexagonal cell vectors  $\mathbf{a}_h$ ,  $\mathbf{b}_h$  and  $\mathbf{c}_h$  are related to the cubic cell vectors of length  $a_c$  by

$$\mathbf{a}_h \approx a_c(0, 1, -1); \quad \mathbf{b}_h \approx a_c(1, -1, 0); \quad \mathbf{c}_h \approx a_c(1, 1, 1)/2.$$

These experiments also suggested that below 50 K there is a distortion of this cell to a pseudo-orthorhombic *C*-centred cell of monoclinic or lower symmetry with the new cell vectors  $\mathbf{a}_t$ ,  $\mathbf{b}_t$ ,  $\mathbf{c}_t$  related to the cubic and hexagonal cell vectors by

$$\begin{aligned} \mathbf{a}_t &\approx a_c(1, 1, -2) \approx 2\mathbf{a}_h + \mathbf{b}_h; & \mathbf{b}_t &\approx a_c(-1, 1, 0) \approx -\mathbf{b}_h; \\ \mathbf{c}_t &\approx a_c(1, 1, 1)/2 \approx \mathbf{c}_h. \end{aligned}$$

These two distortions were reproduced independently in the MDS calculations [13, 14], which indicated that the primitive unit cell of the lowest temperature structure is triclinic with space group  $P\bar{1}$  and  $Z = 3$ . The pseudo-orthorhombic setting ( $\mathbf{a}_t$ ,  $\mathbf{b}_t$ ,  $\mathbf{c}_t$ ) has space group  $C\bar{1}$  with  $Z = 6$ . Although it is not the primitive cell it is convenient to use because the cell angles become equal to 90° in the cubic phase and therefore provide a good measure of the symmetry-breaking distortion [14].

Subsequent attempts to use this information in the analysis of the neutron diffraction data were unsuccessful, and the discrepancy between the neutron and electron diffraction data immediately below the ordering transition at 96 K remained unresolved. High resolution measurements were made with a neutron wavelength of  $\approx 4 \text{ \AA}$  in an effort to split as many unresolved peaks as possible at low scattering angles. Several of these peaks were indeed resolved at this longer wavelength, but the ambiguities in indexing the peaks were not eliminated and the crystal structure remained unsolved.

Recently, during electron diffraction studies of nucleation in supersonic jets [15], a new procedure was developed for the analysis of diffraction data starting from trial structures suggested by considerations of molecular packing [16]. When applied to the neutron diffraction data from SF<sub>6</sub> [10] this procedure succeeded in indexing the diffraction pattern in terms of a cell with triclinic symmetry [17]. The analysis determined the unit cell parameters with sufficient accuracy that a complete refinement became feasible.

In the present paper we report a determination of the detailed crystal structure of SF<sub>6</sub> obtained from new neutron powder diffraction data at 23 K and 85 K. The earlier data at 75 K [10] are also analysed and additional high resolution data at 18 K are presented. The experimental details and results are presented in §§2 and 3. In §4 we consider in more detail the mechanism of the ordering phase transition,

paying attention to the effects of orientational frustration on the molecular packing and the discrepancies between the electron and neutron diffraction results. Finally, in §5 we use the results obtained here to assess and improve the model intermolecular potential that has been used in the MDS calculations.

## 2. Experimental details

The polycrystalline sample of SF<sub>6</sub> was prepared by cryogrinding the condensed gas using the technique reported previously [18]. The sample container was a thin-walled vanadium can of diameter 12 mm and height 70 mm and the sample was 'cold loaded' into a closed-cycle Displex cryostat. The diffraction measurements were made on the C5 triple-axis spectrometer operated in its two-axis mode at the NRU reactor, Chalk River. The monochromator was Si (115), and collimations of 0.44° and 0.20° were used before and after the sample respectively. A sapphire filter (50 mm) was placed in the incident beam to reduce unwanted background. The spectrometer was calibrated using Al powder at room temperature as a standard and the neutron wavelength was 1.48018(2) Å. The experimental profiles were measured by stepping the detector in 0.1° steps from 10° to 120° and typical counting times were 2–3 min per point. For these scans the maximum value of  $\sin \theta/\lambda$  was 0.585 Å<sup>-1</sup>. The powder quality was checked by monitoring the intensity of the strongest Debye–Scherrer peak as a function of specimen orientation around the cylinder axis. The standard deviation from the mean was only 2.5 per cent, showing the powder to be very homogeneous. However, the sample was continuously rotated throughout the measurements to minimize any residual errors due to finite crystalline grain size. The transmission of the sample, measured with the incident beam defined by a narrow slit, was 0.756. The experimental profiles for measurements at 23 K and 85 K are shown in figures 1(a), (b).

The experiments described above used a short wavelength to reach as large a value of  $\sin \theta/\lambda$  as allowed mechanically. But in the use of search procedures to identify the crystal unit cell it is necessary to measure the low angle peaks with the highest possible resolution. Consequently the powder profile of another low temperature sample of SF<sub>6</sub> was measured with a much longer neutron wavelength. These experiments were done on the N5 spectrometer with graphite (0002) as the monochromator. The neutron wavelength in this case was determined by calibration with KCl powder at room temperature as a standard and found to be 4.1037(2) Å. The incident beam was filtered by 15 cm of cold Be to remove higher order contamination. Collimations before and after the sample were 0.44° and 0.20° respectively and the detector was stepped by 0.1° through a range of scattering angles from 20° to 111°. The sample was continuously rotated, and its temperature was 18 K. The experimental profile is shown in figure 2. The maximum value of  $\sin \theta/\lambda$  in this case is 0.201 Å<sup>-1</sup>.

The earlier powder diffraction data at 75 K were measured on the L3 spectrometer with Ge (331) as the monochromator. The neutron wavelength was 1.83377(2) Å with collimations of 0.44°, 0.35° before and after the sample respectively. The maximum value of  $\sin \theta/\lambda$  was 0.421 Å<sup>-1</sup>.

## 3. Results

The crystal structures were refined from the data sets using the powder fitting program EDINP [19]. The triclinic unit cell parameters obtained by Bartell *et al.*

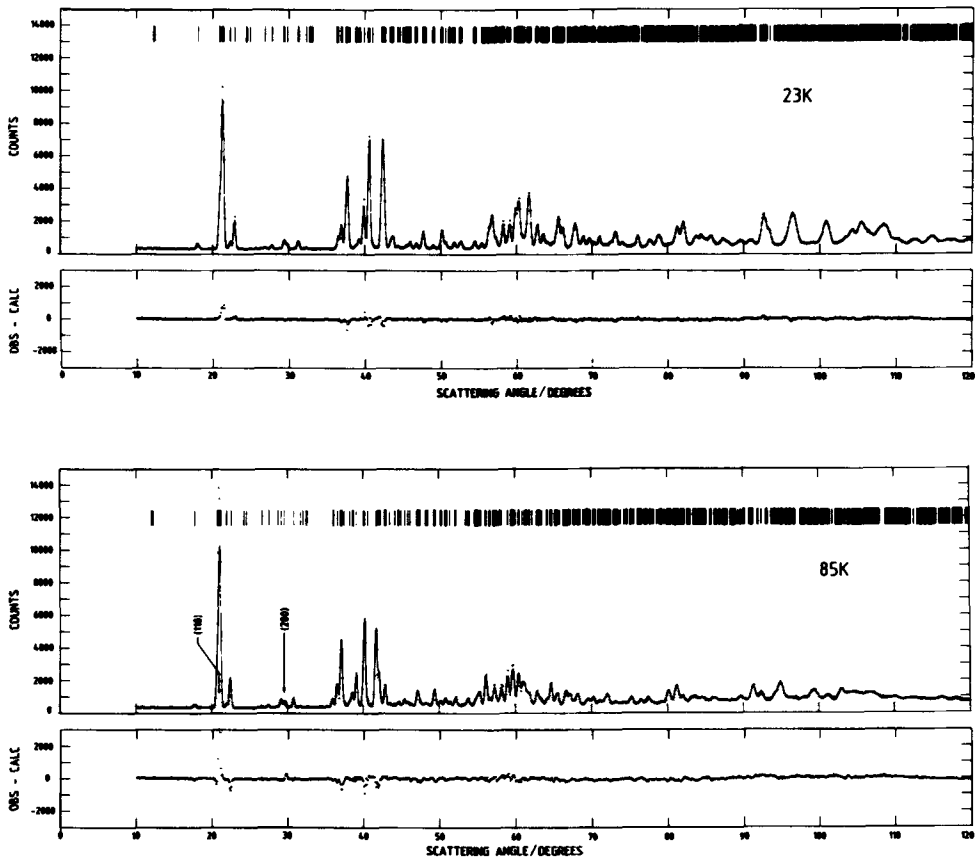


Figure 1. Comparison of the observed and fitted neutron powder profiles of  $\text{SF}_6$  measured with a neutron wavelength of  $1.48018\text{ \AA}$  (a)  $T = 23\text{ K}$ , (b)  $T = 85\text{ K}$ . The vertical tick marks show the positions of individual Debye-Scherrer peaks. The lines marked (111), (200) in (b) show the positions of these peaks for the cubic, high-temperature phase.

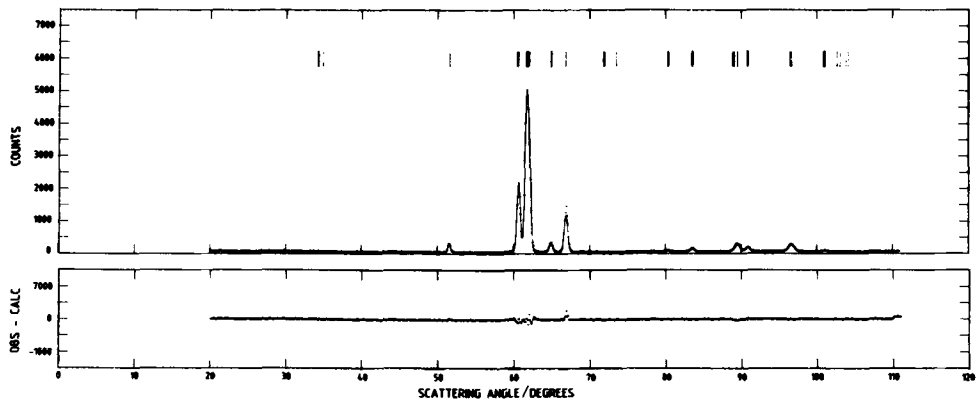


Figure 2. Comparison of the observed and fitted profiles at  $18\text{ K}$  measured with a neutron wavelength of  $4.1037\text{ \AA}$ .

Table 1. The temperature dependence of the structural parameters for the low temperature phase of SF<sub>6</sub>. At 18 K only the unit cell parameters were refined. The Euler angles  $\phi$ ,  $\theta$ ,  $\psi$  are rotations about orthogonal axes X, Y, Z related to crystal lattice axes x, y, z by  $\mathbf{X} // \mathbf{x}$ ,  $\mathbf{Y} // \mathbf{y}$  and  $\mathbf{Z} = \mathbf{X} \times \mathbf{Y}$ . A clockwise rotation is positive.

Temperature (K)	18	75	23	85
Wavelength $\lambda$ (Å)	4.1037	1.83377	1.48018	1.48018
R (per cent)	7.2	7.8	4.9	8.2
Lattice parameters (Å)				
<i>a</i>	14.045(11)	14.140(4)	14.056(2)	14.152(3)
<i>b</i>	8.007(6)	8.091(2)	8.0133(9)	8.105(1)
<i>c</i>	4.752(3)	4.801(1)	4.7548(4)	4.8124(9)
Unit cell angles (deg)				
$\alpha$	85.19(2)	85.55(2)	85.193(5)	85.71(1)
$\beta$	92.73(4)	92.53(2)	92.67(1)	92.48(2)
$\gamma$	89.06(1)	89.14(1)	89.05(1)	89.175(6)
Unit cell volume (Å <sup>3</sup> )	531.81	546.94	532.97	549.87
Euler angles (radians)				
Molecule 1				
$\phi_1$		-2.36(4)	-2.39(3)	-2.35(2)
$\theta_1$		0.55(1)	0.552(4)	0.571(7)
$\psi_1$		2.49(4)	2.63(3)	2.50(2)
Molecule 2				
$\phi_2$		-0.70(1)	-0.680(7)	-0.687(8)
$\theta_2$		-1.02(2)	-1.002(9)	-0.989(9)
$\psi_2$		0.45(1)	0.484(8)	-0.467(8)
S-F bond length (Å)		1.58142(3)	1.56808(9)	1.5799(2)

[17] from the earlier powder diffraction data [10] were used as initial values in the refinements. A primitive unit cell of space group  $P\bar{1}$  with  $Z = 3$  was assumed, but the refinements were performed using the C-centred pseudo-orthorhombic cell ( $Z = 6$ ) described above. The molecules were constrained to have  $O_h$  symmetry, and initial values of the molecular orientations and centre of mass positions were approximately those predicted by the simulations of Pawley and Thomas [14]. The position of one molecule is fixed at the origin of the unit cell on a centre of symmetry while the other two molecules have general positions related by a centre of symmetry. The rigid-body constraint subroutine of EDINP was modified to allow refinement of the S-F bond length and of separate isotropic rigid-body translational and rotational temperature factors for the two independent molecules. The peak widths were defined by the usual  $UVW$  parameters [20], and the asymmetry of the Bragg peaks was modelled using the method proposed by Howard [21] which involves one variable parameter. Three different functions were used to model the background (see below). The total number of variables adjusted in the refinement was thus a maximum of 29: 6 unit cell parameters, 10 structural parameters, 4 temperature factors and up to 9 profile parameters (1 scale, 1 zero angle, 4 peak shape and 1, 2 or 3 background). The results of the refinements with a linear sloping background (see below) are presented in table 1, while table 2 shows the fractional atomic coordinates derived from these parameters. The experimental diffraction patterns are compared with the fitted ones in figures 1(a), (b). The quality of fit is specified by an  $R$ -factor defined as

$$R = \frac{\sum_i |y_i^{\text{obs}} - y_i^{\text{calc}}|}{\sum_i y_i^{\text{obs}}}$$

Table 2. Fractional atomic position coordinates derived from structural parameters of table 1.

Temperature (K)		18	75	23	85	
Molecule 1	x	0	0	0	0	
	S	y	0	0	0	0
		z	0	0	0	0
		x	0.1021	0.1013	0.1010	0.1010
	F	y	-0.0028	-0.0228	-0.0055	-0.0055
		z	-0.1216	-0.1180	-0.1271	-0.1271
		x	0.0216	0.0326	0.0244	0.0244
	F	y	0.1719	0.1653	0.1699	0.1699
		z	0.1231	0.1274	0.1249	0.1249
		x	0.0406	0.0340	0.0412	0.0412
	F	y	-0.0943	-0.1037	-0.0966	-0.0966
		z	0.2819	0.2822	0.2773	0.2773
x		0.3342	0.3346	0.3346	0.3346	
Molecule 2	S	y	-0.0032	-0.0018	-0.0029	-0.0029
		z	0.5913	0.5854	0.5938	0.5938
		x	0.4307	0.4319	0.4319	0.4319
	F	y	-0.0174	-0.0228	-0.0180	-0.0180
		z	0.7719	0.7609	0.7683	0.7683
		x	0.2377	0.2372	0.2373	0.2373
	F	y	0.0111	0.0192	0.0121	0.0121
		z	0.4108	0.4100	0.4192	0.4192
		x	0.2913	0.2965	0.2949	0.2949
	F	y	0.1119	0.1171	0.1172	0.1172
		z	0.8077	0.8026	0.8067	0.8067
		x	0.3771	0.3726	0.3743	0.3743
	F	y	-0.1182	-0.1207	-0.1230	-0.1230
		z	0.3750	0.3683	0.3808	0.3808
		x	0.2969	0.2951	0.2965	0.2965
	F	y	-0.1613	-0.1567	-0.1565	-0.1565
		z	0.7646	0.7640	0.7748	0.7748
		x	0.3715	0.3740	0.3726	0.3726
	F	y	0.1550	0.1531	0.1506	0.1506
		z	0.4181	0.4069	0.4127	0.4127
		x				

where  $y_i^{\text{obs}}$  ( $y_i^{\text{calc}}$ ) are the observed (calculated) intensities at scattering angle  $2\theta_i$ . The refined crystal structure at 23 K is shown in figure 3.

At 23 K there is very good agreement between the observed and fitted diffraction profiles. At 85 K discrepancies are more evident. These are of two kinds: (i) the background, particularly at larger scattering angles, is more intense than at 23 K and is not as well represented by a simple analytic function. (ii) there are discrepancies between observed and fitted peaks at low scattering angles. The positions of the (110) and (200) peaks of the cubic, high-temperature phase are shown in figure 1(b). They clearly occur where there are discrepancies between the observed and fitted profiles. This suggests there is some residual bcc phase present at 85 K, even though this is well below the transition temperature. Since the bcc contamination affects significantly only two low-angle peaks of the  $\approx 900$  peaks in the complete pattern, refinement in terms of the triclinic structure is not greatly affected

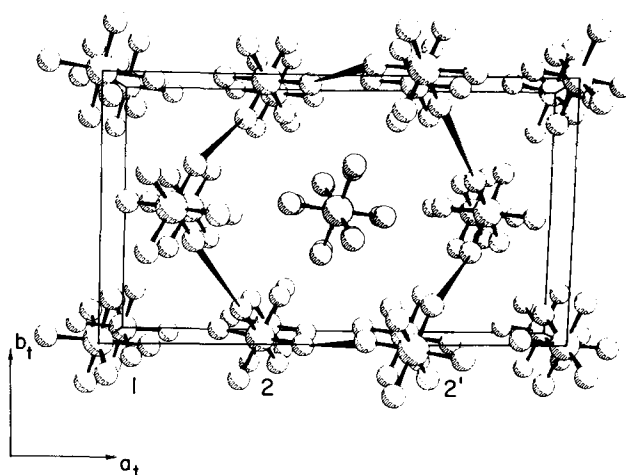


Figure 3. The crystal structure of SF<sub>6</sub> at 23 K derived in the present study. The structure is viewed in perspective down the  $c_1$ -axis. The centres of mass of the molecules have fractional  $z$  coordinates of 0 and 1 (molecule 1),  $\approx -0.4$  and  $\approx 0.6$  (molecule 2) and  $\approx 0.4$  and  $\approx 1.4$  (molecule 2'). The tapered lines between F atoms on different molecules denote the short F...F bonds that lie close to the cubic axes of the disordered phase.

if these two peaks are omitted. The values of the structural parameters obtained with these two peaks included or excluded do not differ by more than their fitted errors. The results given in table 1 were obtained with the peaks excluded.

The diffraction patterns contain too many overlapping peaks to allow direct observation of the background except at low scattering angles. Consequently, three different analytic functions were used to model the background and the data were refined with each one. The first assumption was that of a flat background described by a single adjustable parameter. The second assumption was that of a flat background plus a term increasing linearly with scattering angle. This function is described by two adjustable parameters. The b.c.c. contamination at 85 K, although affecting only a few discrete peaks, will contribute a diffuse background appropriate to the cubic phase. Thus, the third assumption was that of a cubic, diffuse background. Assuming randomly oriented molecules the analytic form is given by equations 2.29, 2.36 and 2.37 of Dolling *et al.* (4). In the notation of that reference it is

$$\text{background} = A + B[(\Delta\beta)^2 + |\langle\beta\rangle|^2\{1 - \exp(-CQ^2)\}],$$

where  $A$ ,  $B$  and  $C$  are adjustable parameters,  $\langle\beta\rangle$  is the rotational structure factor,  $\Delta\beta$  is the equilibrium fluctuation of the molecular scattering amplitude and  $Q = 4\pi \sin \theta/\lambda$ . The assumption of randomly oriented molecules is clearly an oversimplification, but a more exact model would need to include higher order terms and correspondingly more parameters.

For both temperatures the best fit is obtained with the linearly sloping background. The 'diffuse' background and the flat background both give poorer fits. At 23 K the  $R$ -factors are 4.9, 5.7, 6.0 per cent respectively while at 85 K they are 8.9, 11.3, 12.0 per cent with the cubic peaks included and 8.2, 10.4%, 10.3 per cent with

the cubic peaks excluded. Within the fitted errors the structural parameters are the same with either sloping or diffuse background assumptions and are marginally outside these errors for the flat background.

The success of the linear sloping background assumption at 23 K suggests that there must be two contributions to the diffuse background. At high temperatures (e.g. 85 K) b.c.c. contamination will contribute one component. But this will be negligible at 23 K and the sloping background at this temperature must be a second background component due to residual disorder. This suggests that residual orientational disorder may be present even at the lowest temperatures. The cubic, diffuse assumption might be expected to model both these contributions. But the simplified form used here is clearly not appropriate for the ordered phase. The presence of a component of the cubic, disordered phase at 85 K in the ordered low temperature phase is analogous to the co-existence of ordered and disordered phases observed in hexafluoroethane [22]. It suggests that the phase boundaries in these molecular solids may depend on the detailed specimen characterization and history, as well as on temperature.

The earlier data at 75 K [10] show no evidence of contamination with cubic peaks. These data are of lower resolution than the present data and extend over a smaller range ( $\sin \theta/\lambda = 0.421 \text{ \AA}^{-1}$ ). The diffraction pattern was analysed in terms of the triclinic structure described above with the same background assumptions. However, the refinements with the disordered, diffuse background did not converge, probably because any b.c.c. component is too weak to specify adequately the background parameters. The *R*-factors with the sloping and flat backgrounds are 7.8, 10.4 per cent respectively and the values of the structural parameters are also given in tables 1 and 2.

Several points should be noted.

- (1) The refined unit cell parameters are in good agreement with those calculated by Bartell *et al.* [17], the discrepancies are due only to our use of improved individual line profiles.
- (2) It is clear from figure 1 that there is considerable overlap of Debye-Scherrer peaks and several at low angles have such low intensity that they cannot be discerned in the overall diffraction pattern. This explains why conventional analysis of the diffraction pattern failed to yield a solution for the unit cell. The complexity of the structure inevitably results in significant overlap of the lines, for example in the region up to the twentieth observable peak there are 82 Debye-Scherrer lines, and the complete scans in figures 1(a), (b) each contain >900 reflections. An example of the peak overlap is shown in figure 4, where diffraction patterns at different resolution are compared in detail. Even at the best resolution available many of the overlapping peaks cannot be separated.
- (3) The refined structure is very similar to that obtained in the MDS calculations of Pawley and Thomas [14]. This suggests that the choice of the model intermolecular potential used in that and subsequent studies of the phases of SF<sub>6</sub> is valid.
- (4) Refinements were also performed using the lower symmetry space group P1, with three independent molecules in the primitive cell instead of two. No improvement in the fit was obtained, and the symmetry-breaking distortions

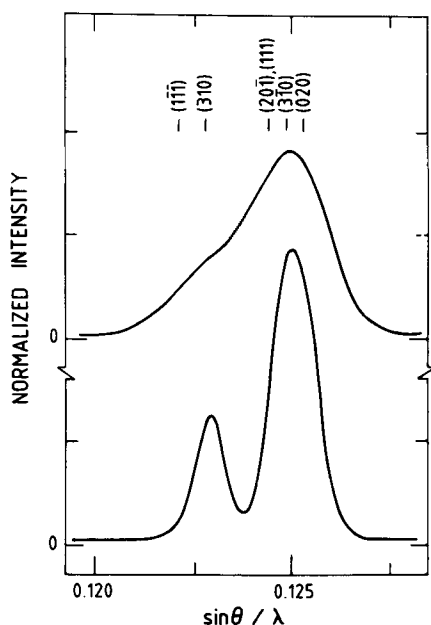


Figure 4. Comparison of the profiles for measurements made with two neutron wavelengths:  $1.48018 \text{ \AA}$  (upper curve) and  $4.1037 \text{ \AA}$  (lower curve). The two profiles have been normalized to show equal integrated intensities, and the solid lines are hand drawn through the data points. The vertical bars indicate the positions of the Debye-Scherrer peaks. The range of  $\sin \theta / \lambda$  extends across the largest peak ( $2\theta \approx 21^\circ$ ) of figure 1(a).

of the structure were negligibly small. Thus we conclude that  $P\bar{1}$  is the correct symmetry of the lowest temperature phase of  $SF_6$ .

- (5) The use of rigid-body isotropic rotational and translational temperature factors intuitively would seem to be a reasonable assumption. However, it was found that these parameters were too highly correlated in the refinements to allow a meaningful interpretation of their values particularly at 85 K and 75 K. This is probably due to the difficulty in modelling the background correctly at large scattering angles for these temperatures. Consequently we do not report the refined values of these parameters.
- (6) No evidence was found for the existence of a partially ordered hexagonal phase intermediate between the triclinic and disordered cubic phases, even though such a phase has been observed in small single crystal samples by electron diffraction [12] and was predicted in simulation calculations [13]. A search for this phase was made by cooling from the cubic phase into the expected temperature regime and also by heating from the triclinic phase, thus eliminating possible hysteresis effects. However, no evidence for the presence of this phase could be found and we must conclude that it does not exist in bulk samples. But such a phase may well represent a possible transition pathway from the cubic to the triclinic phase, so that its existence may be realized under different conditions (e.g. in small samples or with rapid cooling through the transition). This point is discussed further below.
- (7) To provide a further check on our refinements we have performed a fit to the high resolution data shown in figure 2. As the range of  $\sin \theta / \lambda$  is limited

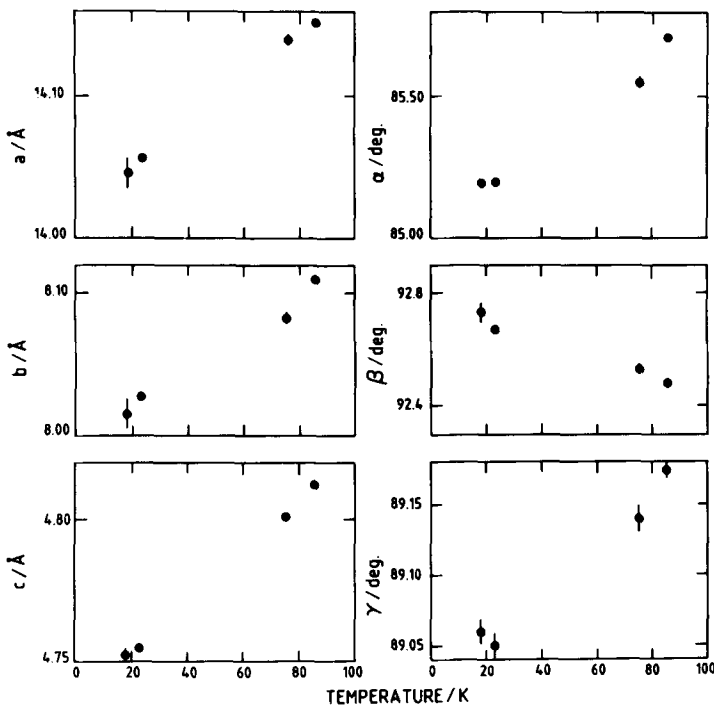


Figure 5. Temperature dependence of the unit cell parameters.

through the use of long wavelength neutrons, we have constrained the structure to be that obtained from the refinement of the lower resolution data at 23 K and have fitted only profile and unit cell parameters. Any small adjustments in the atomic positions would affect the higher angle diffraction peaks only. The results are presented in table 1 and the calculated diffraction pattern is compared with the experimental one in figure 2. As can be seen, the agreement is very good. The temperature dependence of the unit cell parameters is shown in figure 5.

- (8) The errors given in table 1 for the S–F bond length are taken directly from the fitting procedure and are too small to be realistic, a well-known problem in powder profile structure determination. If more realistic errors are assumed then the bond length at 23 K agrees with the value obtained from gas phase electron diffraction measurements [23] and with that from the previous neutron diffraction data in the disordered phase [4]. The bond lengths at 75 K and 85 K agree with each other, but the temperature dependence implied by the relative values at these temperatures and at 23 K does not seem reasonable. This short bond length is determined primarily by the high index reflections. It has been pointed out above that the difficulty in modelling correctly the background at large scattering angles for high temperatures is probably responsible for the difficulty in refining the thermal factors. It is also probably responsible for this discrepancy in the value of the S–F bond length between high and low temperatures.

#### 4. Discussion

The phase transition in SF<sub>6</sub> at 96 K is unusual in that it involves a dramatic lowering of symmetry from cubic to triclinic. Nevertheless, the structures of the two phases are very closely related and it is possible to view the low temperature structure as derived from the cubic structure by small structural distortions which accompany the onset of orientational order. As stated in the introduction, the high temperature b.c.c. structure has two molecules in the cubic unit cell with average molecular orientations that have the S–F bonds lying along the cubic cell axes. In this structure each molecule is coordinated with eight nearest neighbours positioned along  $\langle 111 \rangle$  in favourable (i.e. favouring ordering) relative orientations. It is the packing arrangement for these orientations that yields the b.c.c. structure. However, the price to be paid for this favourable packing is that the next nearest neighbours (positioned along  $\langle 100 \rangle$ ) have unfavourable (i.e. favouring disordering) relative orientations because of overlap repulsion of the nearest fluorine atoms. Thus the molecules must rotate (by  $\approx 20^\circ$ ) to move the S–F bonds away from the cubic axes, dynamically relieving the competition between the ordering nearest neighbour interactions and the disordering next nearest neighbour interactions. We have called this competition ‘orientational frustration’, and it is discussed in more detail in references [6–8].

At low temperatures the molecules no longer have enough kinetic energy to resolve the frustration dynamically and the crystal undergoes the phase transition to the ordered phase. In the ordered phase the volume per molecule is  $\approx 5$  per cent smaller than in the disordered phase. The key feature of the low temperature triclinic phase is that it retains the eight neighbour coordination of the b.c.c. phase with  $\frac{2}{3}$  of the molecules having orientations close to the average orientation of the b.c.c. phase but with small variations. In the structure shown in figure 3 these are the molecules labelled 2 and 2'. In particular it should be noted that in the triclinic structure there are no contacts between fluorine atoms of less than 2.9 Å, whereas for the idealized b.c.c. structure with S–F bonds lying along  $\langle 100 \rangle$  axes the closest contact distance would be about 2.6 Å, although in practice the disorder would rarely allow such short contact distances [7].

It is possible to view the cubic-to-triclinic phase transition as a two stage process. In the first stage the b.c.c. cell transforms to a hexagonal cell with  $Z = 3$ , and with the hexagonal  $c$ -axis lying along a cubic  $\langle 111 \rangle$  direction. The relationship between the hexagonal cell vectors and the cubic cell vectors is given in §1. This hexagonal modulation gives some of the largest distortions from the cubic phase, as seen in the unit cell lengths and the position of molecule 2. Compared with the cubic cell length,  $a_c$ , the triclinic cell lengths  $a_1$ ,  $b_1$ ,  $c_1$  are approximately  $\sqrt{6}a_c$ ,  $\sqrt{2}a_c$  and  $\sqrt{3}a_c/2$ . At 23 K the lengths  $a_1/\sqrt{6}$ ,  $b_1/\sqrt{2}$  and  $2c_1/\sqrt{3}$  are 5.738, 5.666 and 5.490 Å respectively. Since  $a_c = 5.78$  Å at 100 K (4) it is clear that the greatest contraction is along  $c_1$ . In a pseudo-orthorhombic setting of the b.c.c. lattice, molecule 2 would have fractional coordinates of  $\frac{1}{3}$ , 0,  $\frac{2}{3}$ . The actual displacements of molecule 2 from this position at 23 K in the  $a_1$ ,  $b_1$  and  $c_1$  directions are 0.0183, 0.144 and 0.3861 Å respectively, and it is clearly the latter displacement which is the most significant. The contraction and displacement along  $c_1$  are consistent with a large hexagonal distortion. The MDS calculations [13] have shown that this hexagonal distortion will leave the orientation of molecule 1 (at the origin) disordered, while the orientations of the other two molecules in the unit cell will be ordered.

The second stage of the total transformation involves a shear of the hexagonal cell to form the triclinic cell. This is characterized by the three distortion angles  $\Delta_\alpha = \alpha - 90^\circ$  etc, of the pseudo-orthorhombic cell, and at 23 K  $\Delta_\alpha$ ,  $\Delta_\beta$  and  $\Delta_\gamma$  are  $-4.81^\circ$ ,  $2.67^\circ$  and  $-0.95^\circ$  respectively. As  $\Delta_\gamma$  is significantly smaller than the other two distortions we suggest that the primary distortion is not a shear within the hexagonal basal plane (the triclinic *a-b* plane) but involves a shear perpendicular to this plane. Noting that the ratio  $-\Delta_\alpha/b_t$  is approximately three times greater than the ratio  $\Delta_\beta/a_t$ , we surmise that this shear involves a tilting of the hexagonal *c*-axis towards the triclinic  $[\bar{1}\bar{3}0]$  direction, which is the hexagonal  $[\bar{1}10]$  direction. By combining  $\Delta_\alpha$  and  $\Delta_\beta$  we find a shear angle of  $5.5^\circ$  at 23 K and  $5.0^\circ$  at 85 K. The shear in the  $a_t$ - $b_t$  plane ( $\Delta_\gamma$ ) follows as a second order effect. This analysis is consistent with calculations of the rotation of molecule 2 from an idealized b.c.c. orientation defined with respect to three orthogonal axes with one lying along the  $a_t$  axis and another in the  $a_t$ - $b_t$  plane: the rotations about the  $a_t$ ,  $b_t$  and  $c_t$  axes are  $-4.84^\circ$ ,  $2.93^\circ$  and  $-1.18^\circ$  respectively, which are similar in value to the distortions  $\Delta_\alpha$  etc.

Thus we conclude that the cubic-to-triclinic distortion involves two instabilities, namely a contraction along a cubic  $\langle 111 \rangle$  direction to form a hexagonal intermediate structure, followed by a shear of the intermediate structure towards an hexagonal  $[\bar{1}10]$  direction. We have argued elsewhere [13] on the basis of MDS calculations that these two stages also involve different ordering processes. The first stage is associated with ordering of the orientations of  $\frac{2}{3}$  of the molecules (2 and 2'), which is caused by the attractive nearest neighbour interaction and which also leaves molecule 1 (at the origin) with more orientational freedom. The second stage is then associated with the ordering of the remaining molecules. Since we did not observe the hexagonal phase, it appears from our experiments that both stages occur together at the first order transition at 96 K. However, the possibility of b.c.c. contamination below the transition and the consequent diffuse background, as observed in the 85 K data (and to a lesser extent at 23 K) and the disorder seen in the MDS calculation at 80 K [13] all suggest that at temperatures even well below the transition not all molecules are necessarily orientationally ordered. Consequently, it is not unreasonable to suppose that in small samples or at surfaces the internal strain may not be strong enough to stabilize the shear distortion of the triclinic phase and the hexagonal phase might then be metastable in some temperature range. Thus the electron diffraction [12] and MDS [13] results are not inconsistent with the findings of the present study.

### 5. A model inter molecular potential

In the MDS calculations for  $\text{SF}_6$  the intermolecular potential was modelled [6-9, 13, 14, 24] using a simple Lennard-Jones potential for pairwise atom-atom interactions between fluorine atoms only

$$V(r_{ij}) = -4\varepsilon[(\sigma/r_{ij})^6 - (\sigma/r_{ij})^{12}],$$

where  $r_{ij}$  is the distance between the  $i$ th fluorine atom of one molecule and the  $j$ th fluorine atom of a different molecule; the total interaction is the complete summation over  $i$  and  $j$ . The parameter  $\varepsilon$  defines an energy scale, so that at temperatures close to 0 K the crystal structure obtained with the model is determined only by the value of  $\sigma$ . Explicit interactions involving the sulphur atoms were neglected, for it was assumed that the effects of such interactions would be to modify the values of  $\varepsilon$

and  $\sigma$  for the F...F interactions. Similarly, electrostatic interactions were not included in the model as these are expected to be relatively weak and of short range due to the high symmetry of the SF<sub>6</sub> molecule.

We can now use the low temperature structure of SF<sub>6</sub> to assess and improve this potential model, which was developed on the basis of the idealized structure of the high temperature disordered phase [24]. We have used the energy minimization program WMIN [25] to adjust the value of  $\sigma$ . This was found by minimization of the residual

$$M = \sum_i (\partial W / \partial P_i)^2,$$

where  $W$  is the lattice energy and  $P_i$  represents any of the 15 structural parameters whose values are not determined by symmetry. A value of  $\sigma = 2.8591 \text{ \AA}$  was obtained, compared with  $\sigma = 2.7 \text{ \AA}$  used in the simulations [6, 24]. The latter value was obtained from the measured cell parameter and an estimated value for the sublimation energy. This small (6 per cent) increase in  $\sigma$  is consistent with the previous observation [6, 8] that the parameters used in the MDS calculations apparently gave a potential that is softer than the real one. The value of  $\sigma = 3.024 \text{ \AA}$  suggested by Powles *et al.* [26] from analysis of gas phase data deviates from our revised value as much as that used in the simulations, although it differs from the old value in the correct direction.

We have attempted to extend the above simple model to incorporate S...S and S...F interactions by using WMIN to find appropriate values for the potential parameters. Although the residual  $M$  was reduced in the fitting procedure, the minimization yielded unphysical values for all parameters. This suggests that the effects of the sulphur interactions are no more significant than departures from the isotropic nature of the atom-atom model, so that it is a reasonable approximation to neglect them.

We have allowed the experimental low-temperature structure to relax in order to minimize the calculated lattice energy, using both new and old values of  $\sigma$ . The results of these minimizations are shown in table 3. Both sets of relaxed structural parameters are in reasonable agreement with the experimental values, but the new value of  $\sigma$  does give smaller discrepancies.

Since we are using a one-parameter model ( $\sigma$  is the only effective parameter at  $T \approx 0$ ) to seek agreement with 15 structural parameters, the quality of the agreement is excellent. The results for the old potential do not exactly match the unit cell parameters reported by Pawley and Thomas [14] from their simulation results. But their cell parameters were taken from the centre of a large crystallite and were not space or time averaged and so the discrepancy is probably not significant. We conclude from the above discussion that the simple potential model which has been used in the simulations can, with only slight modification of the parameter values, account fully for the details of the low temperature ordered structure of SF<sub>6</sub>.

## 6. Conclusions

The crystal structure of the low temperature ordered phase of SF<sub>6</sub> has been solved from neutron powder diffraction data. Along with CDBr<sub>3</sub> [27] it is the lowest symmetry structure yet solved by this technique. The large symmetry change from cubic to triclinic can be understood in terms of two lattice distortions that

Table 3. Results of the lattice relaxation procedure described in the text using two values of the potential parameter  $\sigma$  and starting from the refined structure at 23 K. The results for the unit cell parameters ( $\alpha$ - $\gamma$ ) are shown as the changes from the refined values of table 1. The orthogonal rotations ( $r_x$  etc.) and translations ( $t_x$  etc.) show the changes in the structure following minimization of the lattice energy.  $\Delta W$  is the fractional change in lattice energy (the absolute value depends on the undetermined parameter  $\epsilon$ ).  $\Delta_h$  gives the measure of the intermediate hexagonal distortion as described in the text, and is defined as  $\Delta_h = 100 \times (a + \sqrt{3}b - \sqrt{2}c)/(a + \sqrt{3}b)$ .  $\theta_1$  gives a measure of the triclinic shear modulation defined in the text, and is given by  $\theta_1 = [(90 - \alpha)^2 + (90 - \beta)^2]^{1/2}$ .

Parameter	$\sigma = 2.70 \text{ \AA}$	$\sigma = 2.8591 \text{ \AA}$
$a$ (Å)	-0.502	-0.017
$b$ (Å)	-0.327	-0.035
$c$ (Å)	-0.171	-0.006
$\alpha$ (deg)	-0.367	-0.180
$\beta$ (deg)	0.259	0.158
$\gamma$ (deg)	-0.834	-0.615
Molecule 1		
$r_x$ (deg)	1.78	1.32
$r_y$ (deg)	-2.49	-0.51
$r_z$ (deg)	-0.47	1.95
Molecule 2		
$r_x$ (deg)	-0.24	-1.59
$r_y$ (deg)	-1.09	-0.60
$r_z$ (deg)	-0.15	-0.40
$t_x$ (Å)	-0.0082	-0.0083
$t_y$ (Å)	-0.0026	-0.0033
$t_z$ (Å)	-0.0509	-0.0380
$\Delta W$ (per cent)	8.40	0.69
$\Delta_h$ (per cent)	3.48	3.55
$\theta_1$ (deg)	5.146	5.734

couple to two ordering processes involving different molecules. Thus the apparent inconsistencies between structural data obtained by different techniques can be partially understood. The disordering mechanism in the cubic high temperature phase is orientational frustration. As the temperature is lowered through the transition the distortions from the cubic phase are consistent with the resolution of this frustration being the driving mechanism of the transition. The results are in agreement with molecular dynamics simulation calculations and thus add weight to the validity of the intermolecular potential model used in the simulations. They have also shown the considerable predictive power of such simulations. The results obtained here have been used to improve the intermolecular force model used in the simulations.

One of the authors (M.T.D.) thanks SERC (U.K.) for supporting a stay in Chalk River and thanks the staff of Atomic Energy of Canada Limited for their kind hospitality during this visit. Gerald Dolling participated in the early measurements and Peter Gerlach assisted with the high resolution measurements. The authors thank J. C. Evans for his technical expertise in preparing the sample.

*Note added in proof.*—It has been brought to the attention of the authors that the triclinic cell described in the present paper may be reduced and described in terms of a higher symmetry monoclinic cell with space group  $C2/m$  (COCKROFT, J. K., and FITCH, A. N., 1987, *Science*, N.Y. (to be published)). The structure reported here is equivalent to that with space group  $C2/m$  and departures from this higher symmetry are negligibly small. The conclusions drawn from our refinements with space group  $P\bar{1}$  are therefore unaffected by the description of the structure in terms of the higher symmetry space group. We shall publish a short note expressing our results in terms of the higher symmetry cell.

### References

- [1] EUCKEN, A., and SCHRÖDER, E., 1938, *Z. phys. Chem.*, **B41**, 307.
- [2] MICHEL, J., DRIFFORD, M., and RIGNY, P., 1970, *J. Chim. phys.*, **67**, 31.
- [3] GARG, S. K., 1977, *J. chem. Phys.*, **66**, 2517.
- [4] TAYLOR, J. C., and WAUGH, A. B., 1976, *J. Solid State Chem.*, **18**, 241. DOLLING, G., POWELL, B. M., and SEARS, V. F., 1979, *Molec. Phys.*, **37**, 1859.
- [5] POWELL, B. M., SEARS, V. F., and DOLLING, G., 1982, *Neutron Scattering—1981*, edited by J. Faber, Jr. (AIP #89), p. 221.
- [6] DOVE, M. T., and PAWLEY, G. S., 1983, *J. Phys. C*, **16**, 5969.
- [7] DOVE, M. T., and PAWLEY, G. S., 1984, *J. Phys. C*, **17**, 6581.
- [8] DOVE, M. T., PAWLEY, G. S., DOLLING, G., and POWELL, B. M., 1986, *Molec. Phys.*, **57**, 865.
- [9] DOVE, M. T., and LYNDEN-BELL, R. M., 1987, *Dynamics of Molecular Crystals*, edited by J. Lascombe (Elsevier), p. 705.
- [10] POWELL, B. M., DOLLING, G., EVANS, J. C., and NIEMAN, H. F., 1980, AECL Report No. 7055 (unpublished data).
- [11] LOUER, D., and LOUER, M., 1972, *J. appl. Crystallogr.*, **5**, 271.
- [12] RAYNERD, G., TATLOCK, G. J., and VENABLES, J. A., 1980, *Acta crystallogr. B*, **38**, 1896.
- [13] PAWLEY, G. S., and DOVE, M. T., 1983, *Chem. Phys. Lett.*, **99**, 45.
- [14] PAWLEY, G. S., and THOMAS, G. W., 1982, *Phys. Rev. Lett.*, **48**, 410.
- [15] BARTELL, L. S., VALENTE, E. J., and CAILLAT, J. C., 1987, *J. phys. Chem.*, **91**, 2498.
- [16] CAILLAT, J. C., and BARTELL, L. S., 1986, *Quant. Chem. Prog. Exch.*, program 520, Indiana University, Bloomington, Indiana 47405.
- [17] BARTELL, L. S., CAILLAT, J. C., and POWELL, B. M., 1987, *Science*, N.Y., **236**, 1463.
- [18] NIEMAN, H. F., EVANS, J. C., HEAL, K. M., and POWELL, B. M., 1984, *J. appl. Crystallogr.*, **17**, 372.
- [19] PAWLEY, G. S., 1980 *J. appl. Crystallogr.*, **13**, 630.
- [20] RIETVELD, H. M., 1969, *J. appl. Crystallogr.*, **2**, 625.
- [21] HOWARD, C. J., 1982, *J. appl. Crystallogr.*, **15**, 615.
- [22] POWELL, B. M., PRESS, W., DOLLING, G., and SEARS, V. F., 1984, *Molec. Phys.*, **53**, 941.
- [23] BARTELL, L. S., and DOUN, S. K., 1978, *J. molec. Struct.*, **43**, 245. GOATES, S. R., and BARTELL, L. S., 1982, *J. chem. Phys.*, **77**, 1866.
- [24] PAWLEY, G. S., 1981, *Molec. Phys.*, **43**, 1321.
- [25] BUSING, W. R., 1981, internal report ORNL-5747, Oak Ridge National Laboratory.
- [26] POWLES, J. G., DORE, J. C., DERAMAN, M. B., and OSAE, E. K., 1983, *Molec. Phys.*, **50**, 1089.
- [27] MYERS, R., TORRIE, B. H., and POWELL, B. M., 1983, *J. chem. Phys.*, **79**, 1495.